

# The Calculated Justification of Seismic Stability of Load-Lifting Cranes

NIKOLAI PANASENKO <sup>(1)</sup>,  
ALEKSEI SINELSHCHIKOV <sup>(2)</sup>,  
VADIM RABEY <sup>(3)</sup>

Lifting-and-Transport Machines, Industrial Logistics and Mechanics of Machines  
Astrakhan State Technical University  
414025, Russia, Astrakhan, St. Tatishcheva, 16  
RUSSIA

<sup>(1)</sup>psastr@mail.ru; <sup>(2)</sup>laex@bk.ru; <sup>(3)</sup>vadimbey@hotmail.com

*Abstract:* - To provide seismic safety for engineering structures remains a prevalent problem. In particular, attention is given to facilities whose destruction can cause damage to the population and the environment, such as the facilities that use nuclear energy. According to the maps of the general seismic regionalization OSR-97, independent spent fuel storage installation (ISFSI) with crane loadings of mining and chemical plant (MCP) (Zheleznogorsk, Krasnoyarsk Territory, Russian Federation) was related to 7 magnitude zones according to the MSK-64 scale. To justify the seismic safety using FEA, a dynamic spatial model of the MCP's building was developed, which includes bridge cranes with lifting capacities of 160/32 t, 16/3.2 t and 15 t. The model was used for the floor accelerogram plotting at elevation marks of the cranes' installment at +23 m, +16.8 m and +8.55 m and for the strength calculation of the supporting systems of the building using the dynamic analysis method (DAM) and the linear-spectral method (LSM). The equations of motion with multiple degrees of freedom of the dynamic model were solved using the numerical Gear method and the linear-spectral method (LSM). Based on the calculated floor accelerograms, the probability model of the seismic action was built in the form of probability-statistical floor accelerograms for the elevation marks of the cranes' installment. The stress-strain state of the building and the bridge cranes was calculated under the seismic action conditions. The development of the LSM theory was proposed for the spatial constructions of industrial buildings with crane loadings. The efficiency of the proposed calculated methodology was established, and this proposed methodology was tested in the industrial sphere of a facility with nuclear energy usage that conforms to tightened seismic safety standards.

*Key-Words:* - Seismic safety, Industrial buildings, Load-lifting cranes, Earthquake accelerograms, Equations of motion, Stress-strain state

## 1 Introduction

The mining and chemical plant (MCP) (Zheleznogorsk, Krasnoyarsk Territory, Russian Federation) is a nuclear energy facility (FUNEL), whose aseismic design, construction and use of buildings, structures and technological and crane equipment are regulated by the SNiP II-7-81\* "Construction in earthquake-prone regions" [1] building code and normative documents [2,3]. In these normative documents, updated maps of the general seismic regionalization are included from the OSR-97 map set. All facilities of the MCP were erected prior to the publication of the OSR-97 maps (Fig. 1), and until 1998, they were considered seismically safe by the Russian Academy of Sciences (RAS) [4]. According to the valid OSR-68 and OSR-78 at that time of the general seismic regionalization of USSR territory, no seismic stability was required for the facilities of the MCP

because the plant facilities that appeared in the OSR-78 map were situated in the 5.0 magnitude zone.

According to NP 031-01 [3], which has been developed according to federal standards and rules in the sphere of nuclear energy usage, the general seismic regionalization maps in the territory of the Russian Federation (OSR-97) and the recommendations of International Atomic Energy Agency (IAEA) (№ 50-SG-D15, Vienna, 1992 and № 50-SG-S1, Vienna, 1994), the seismic danger around the MCP is determined from the OSR-97D map for maximum credible earthquake (MCE) (see Fig. 1). The OSR-97D map meets 99.5% probability of not exceeding (or 0.5% possible exceeding) in the course of 50 years of the predicted seismic intensity of shaking in magnitude. According to SNiP II-7-81\*[1], for the average soil conditions of the 2<sup>nd</sup> category, this result corresponds to magnitude 6.1

for planned earthquake (PE) and magnitude 7.5 for MCE.

According to NP 061-05 [2], NP 043-03 [5] and NP 031-01 [3], nuclear and radiation safety requirements concerning the storage and the transportation of spent nuclear fuel (SNF) must be added with the FUNE seismic safety under the MCE conditions of magnitude 7.0 on the MSK-64 scale. Therefore, according to NP 016-05 [6], the MCP industrial building of independent spent fuel storage installation (ISFSI) belonged to the 1<sup>st</sup> category of

seismic stability fixed structures intended for transportation, transfer and storage of nuclear materials. Thus, by the order of MCP and the leading research institute "VNIPIET" JSC (St. Petersburg), the authors of this study performed a calculated justification of the seismic stability of the load-lifting cranes of ISFSI of MCP. The study was performed by passing through its subgrade MCE of magnitude 7.0, which was developed by the Institute of Geoecology of RAS [4] (see Fig. 2), which considered the requirements of RB 006-98 [7].

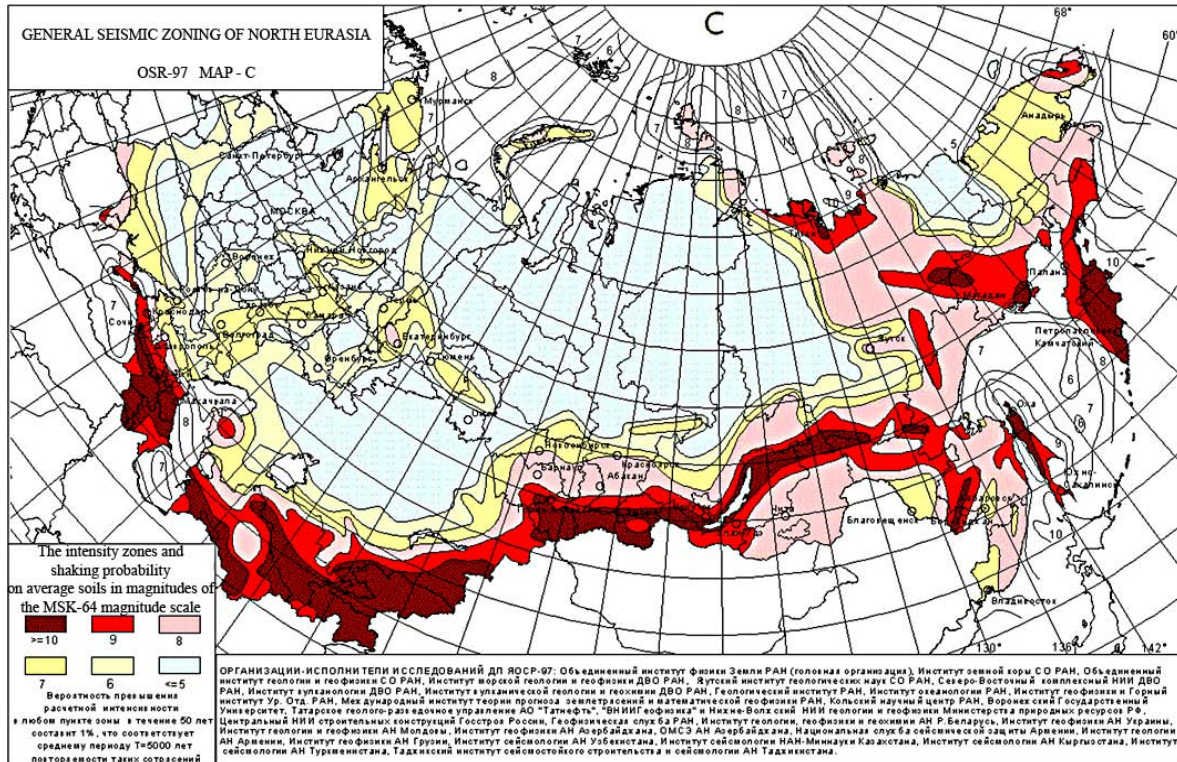


Fig. 1 - General seismic zoning map (OSR-97C) of North Eurasia

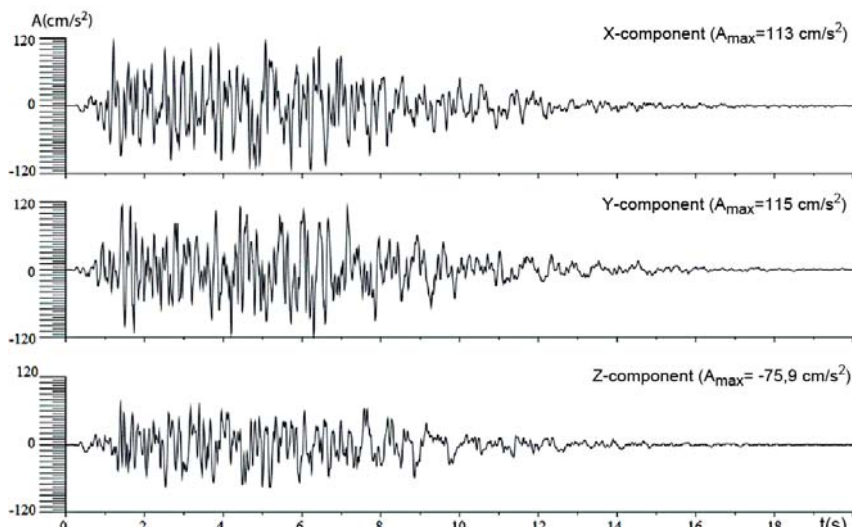


Fig. 2- Synthetic three-component accelerogram (digitized on a time line of 20 sec) of the MCE of magnitude 7.0 on an earth surface, which considers the vertical seismic profile of thickness of the earth under the foundation of the ISFSI building № 1[4]

## 2 Problem Definition

The following tasks had to be solved for the calculation analysis of the seismic safety of ISFSI: 1) conformable elaboration of the principal provisions of seismic stability theory to combine the action of the supporting structures of the storage building with a system of transportation and storage of containers (100-120 ton) with SNF in the wet storing pool [8, 9]; 2) development of a dynamic model of the combined system of the ISFSI industrial building considering the bridge cranes; 3) development of a mathematical model of the ISFSI seismic vibrations as a differential equation-of-motion system with many degrees of freedom (in this case,  $n=46207$ ) based on the nonlinear theory of finite element method (FEM) and solving it using the dynamic analysis method (DAM) by numerically integrating the seismic equation-of-motion system; 4) development of a probability model for the floor seismic load (SL) on the lifting equipment in accordance with the elevation mark of its installment on the runway rails; 5) development of a dynamic model of four types of load-lifting bridge cranes in service using different types of loose gears (LG); 6) calculation analysis of the seismic stability of the load-lifting bridge cranes in the process of SNF transfer under the operation of the SL DAM probability model by numerically integrating the seismic equation-of-motion system with many degrees of freedom.

## 3 Mathematical Model of Floor Accelerograms on the DAM Basis

The dynamic model of the ISFSI building is a discrete-continuum shell-beam system with  $n=46207$  degrees of freedom, which includes 6601 nodes and 10660 finite elements (FE) (Figs. 3 and 4). In the meshing of the ISFSI building, the following nodes have been taken: 1) intersection points of the beams' axes; 2) bend points of the beams' axes; 3) points of joining of support connections; 4) end free points of cantilever constructions; 5) points where an abrupt change of physical or geometrical properties of the constructional elements occurs; 6) points of application of concentrated forces and moments; 7) points of distributed load; 8) all points where the deformation values and the components of the internal forces were necessary to determine.

According to FEM, the finite-element equations of motion with  $n$  degrees of freedom (1) of the ISFSI dynamic model are given by

$$[M]\{\ddot{V}\} + [C]\{\dot{V}\} + [K]\{V\} + \{R(V, \dot{V})\} = \{P\}, \quad (1)$$

where  $[M, C, K]$  are the mass matrix, the damping matrix and the stiffness matrix of the calculation elements of the building;  $\{V\}$  is the displacement vector of the  $n$ th-order (and its first- and second-order derivatives);  $\{P\}$  is the load vector, which accounts for a dead weight of the elements of the dynamic model, the technological loads and three component seismic loads  $[M] \times \{(\cos)\ddot{A}(t)\}$ , where  $\ddot{A}(t)$  is an accelerogram (see Fig. 2) that is set by digitization; and  $\{\cos\}$  is the direction cosine vector of SL with respect to the axes of the global coordinate system (GCS) of the ISFSI dynamic model (see Figs. 3 and 4).

To integrate the seismic equation-of-motion system (1) in the present study, the absolutely stable method of Gear was used in the form of backward differentiation formulas [10, 11]. This method allows for the control of the derivative sign of  $\partial f / \partial y$  at each integration step and effectively builds an integration algorithm for the system of differential equations (1). The Gear method is more advantageous than other numerical integration methods of differential equation-of-motion systems. To prove this advantage, the authors accumulated considerable amounts of information about the reasonability of using this method to solve the dynamic analysis problems of the finite element method [12].

According to the Gear method, the matrix equation of motion (1) is transformed into the  $2n$ th-order equation system of the form

$$\begin{cases} [E]\{\dot{W}\} = \{W\}; \\ [M]\{\dot{W}\} = -[C]\{W\} - [K]\{V\} - \\ -\{R(V, \dot{V})\} + \{P\} \end{cases}, \quad (2)$$

where  $[E]$  is the identity matrix. Considering the phase coordinates vector (3)

$$Y = \{\{V\}, \{\dot{V}\}\}^T = \{\{V\}, \{W\}\}^T, \quad (3)$$

system (2) is written as

$$[D]\{\dot{Y}\} = [B]\{Y\} + \{H\}, \quad (4)$$

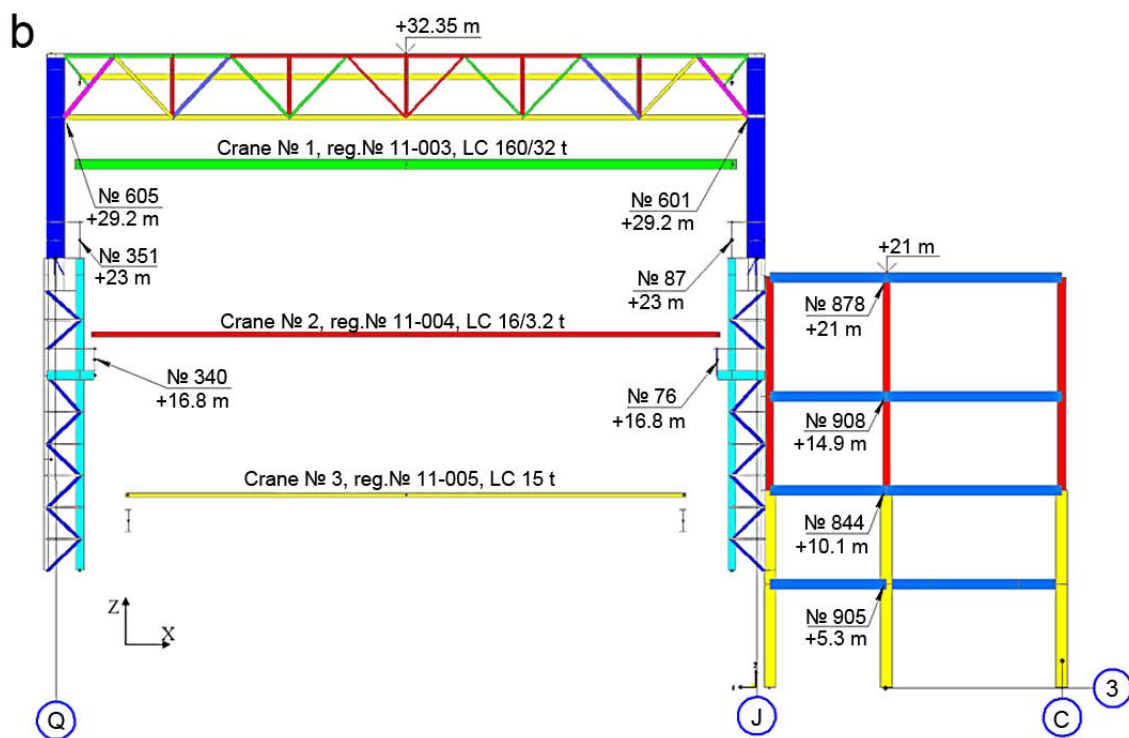
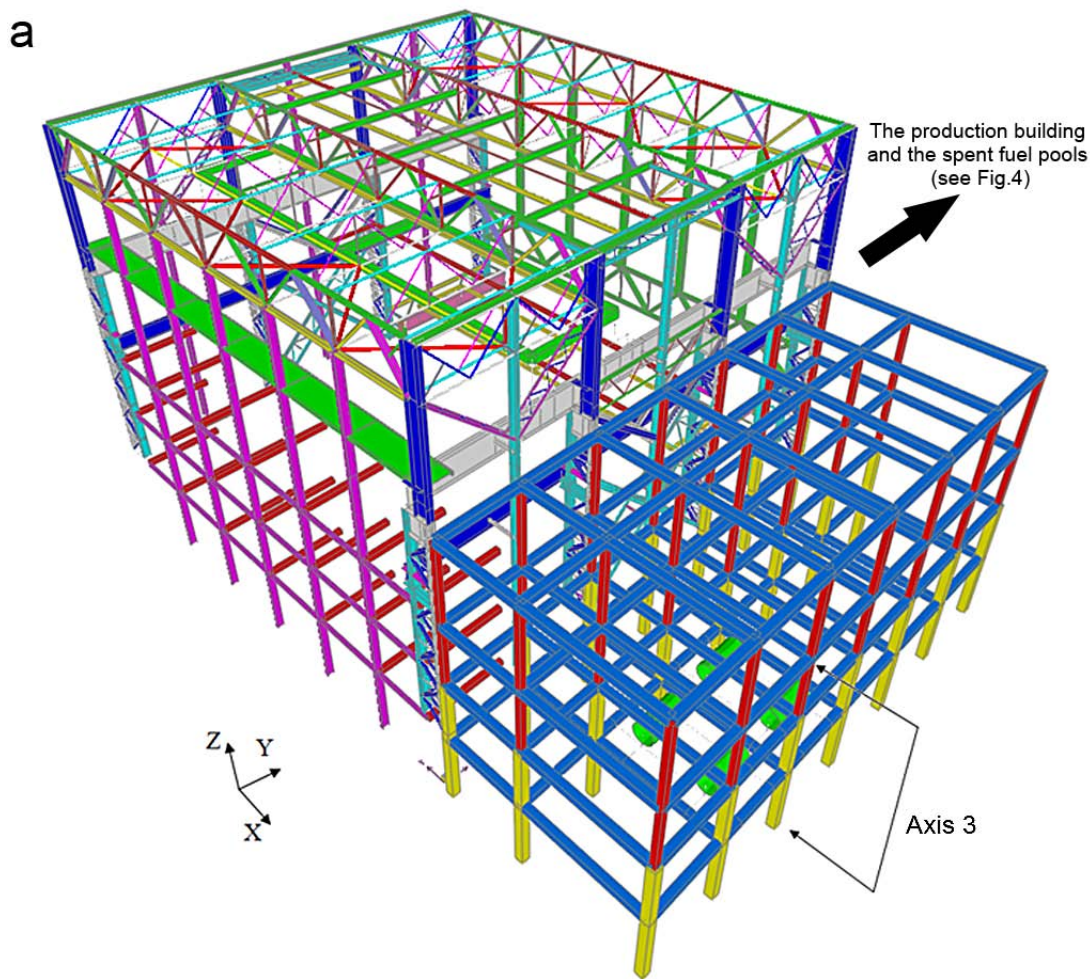


Fig. 3 - Dynamic model of the receiving department of the ISFSI building № 1 of MCP: a – the general appearance of the dynamic model; b – axis 3, on which 15-ton, 16/3.2-ton and 160/32-ton bridge cranes are situated

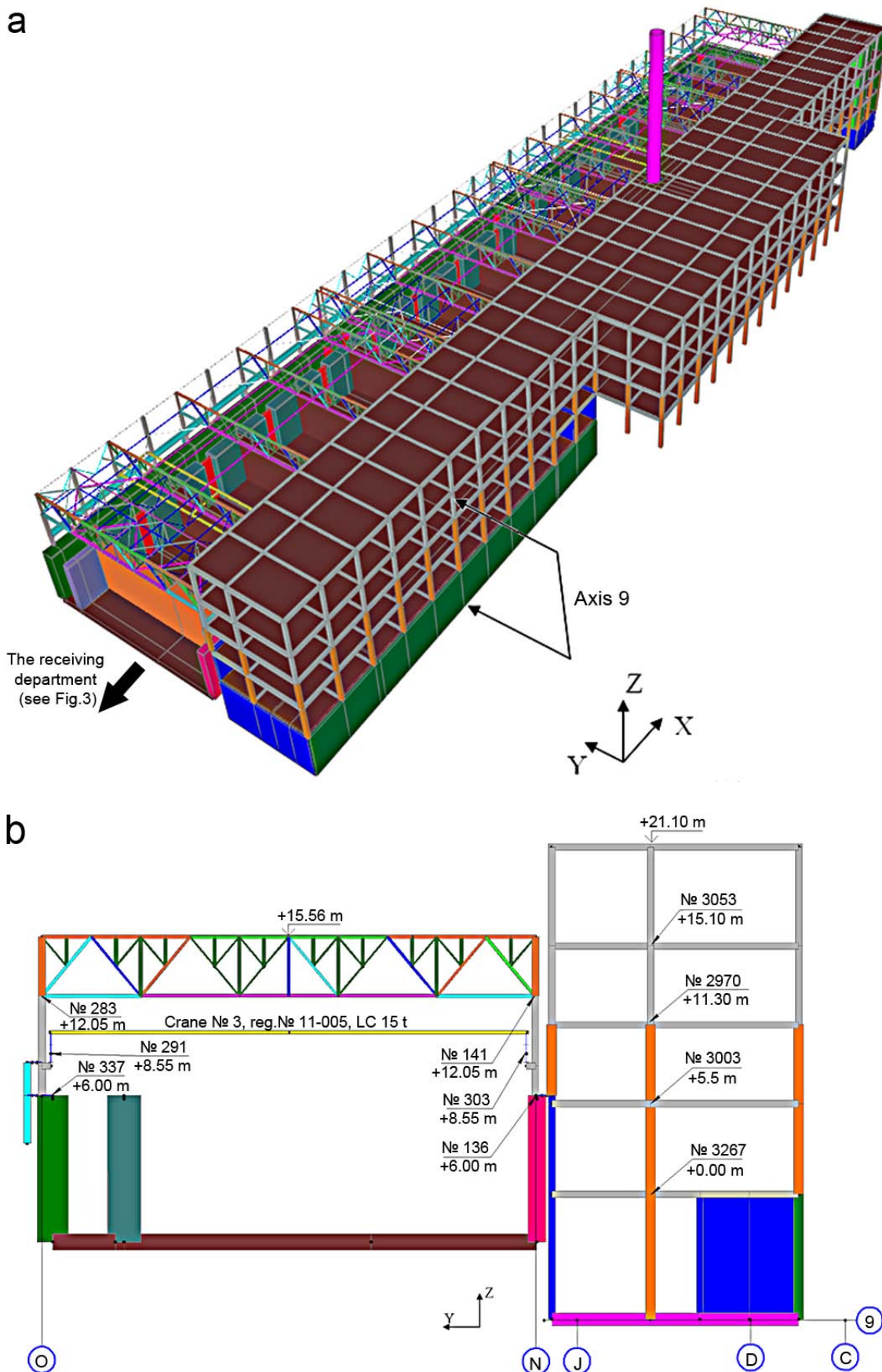


Fig. 4- Dynamic model of the production building and the spent-fuel pools of ISFSI building № 1 of MCP: a - the general appearance of the dynamic model; b – axis 9, on which a 15-ton bridge crane is situated

or in the expanded form ( $W_i = \ddot{V}_i, i > 1, 2, \dots, n$ )

$$\begin{bmatrix} [E] & [0] \\ [0] & [M] \end{bmatrix} \begin{Bmatrix} \{\dot{V}\} \\ \{\dot{V}\} \end{Bmatrix} = \begin{bmatrix} [0] & [E] \\ -[K] & -[C] \end{bmatrix} \begin{Bmatrix} \{V\} \\ \{\dot{V}\} \end{Bmatrix} + \begin{Bmatrix} 0 \\ \{P\} - \{R(V, \dot{V})\} \end{Bmatrix} \quad (5)$$

As opposed to the one-step methods, in (5), it is not necessary to compute  $[M]^{-1}$  to substantially increase the accuracy of a computation. The solution of equation (4) is obtained in the form of an iterative convergent process:

$$\begin{aligned} Z_n^{(0)} &= PZ_{n-1}; \\ Z_n^{(v+1)} &= Z_n^{(v)} - IWF(Z_n^{(v)}), \end{aligned} \quad (6)$$

where  $Z_n$  is the Nordsieck vector [11], which is presented in the transposed (T) form as follows:

$$\begin{aligned} Z_n &= [\{Y\}^n, h\{\dot{Y}\}^n, \frac{1}{2}h^2\{\ddot{Y}\}^n, \frac{1}{6}h^3\{\ddot{\ddot{Y}}\}^n, \dots \\ &\dots, \frac{1}{k!}h^k\{Y^{(k)}\}^n]^T. \end{aligned} \quad (7)$$

In (6) and (7),  $k$  is the order of the Gear method (the maximum number of the first terms of the Taylor series of the obtained solution that coincides with an exact solution of the differential equation of motion);  $P$  is the Pascal triangular matrix of the  $2n$ th-order:

$$P = \begin{bmatrix} 1 & 1 & 1 & 1 & 1 & \dots & 1 \\ & 1 & 2 & 3 & 4 & \dots & k \\ & & 1 & 3 & 6 & \dots & \frac{k(k-1)}{k} \\ & & & \dots & \dots & \dots & \dots \\ & & & & 1 & \dots & \frac{k(k-1)}{k} \\ & 0 & & & & 1 & k \\ & & & & & & 1 \end{bmatrix}, \quad (8)$$

$I$  is a vector of the form  $\{I\} = \{I_0, I_1, \dots, I_k\}^T$  with constant coefficients that depend on the order of the Gear method, as shown in Table 1. In formula (6),  $F(Z_n^{(v)})$  is the residual function:

$$F(Z_n^{(v)}) = hF(x_n, (\{Y\}^n)^{(v)}) - h(\{\dot{Y}\}^n)^{(v)}. \quad (9)$$

Here,  $(\{Y\}^n)^{(v)}$  and  $(\{\dot{Y}\}^n)^{(v)}$  are the solutions that were obtained at the  $v$ th iteration step. Moreover, in (6),  $W$  is the iteration matrix of the form

$$W = \left( \frac{\partial F(Z_n^{(v)})}{\partial Z} \cdot I \right)^{-1}. \quad (10)$$

Table 1. Constant coefficients that depend on the order of the Gear method.

Coefficients	kth-order of the Gear method				
	2	3	4	5	6
$i_0$	2/3	6/11	12/25	60/137	20/49
$i_1$	1	1	1	1	1
$i_2$	1/3	6/11	7/10	225/274	58/63
$i_3$		1/11	1/5	85/274	5/12
$i_4$			1/50	15/274	25/252
$i_5$				1/274	1/84
$i_6$					1/1764

Obviously, if the right-hand side of equation (4) is linear as a result of not considering the dry frictional forces of the locked travelling wheels of cranes on the runway rails and the geometric nonlinearity, which is given in equation (1) ( $\{R(V, \dot{V})\} = 0$ ), then the iterative process (6) converges in one iteration. Moreover, the Gear method can control the miscalculations at each step, which allows it to build adaptive computational processes with an automatic integration step selection and order of integration scheme that allows for solving linear and nonlinear problems of dynamic analysis. According to the computational analysis results of the seismic vibrations for the receiving department of ISFSI building № 1 of MCP 47, which was digitized on a timeline of 20 sec, the three-component seven-axis floor accelerograms were obtained at elevation marks of +5.3 m, +10.1 m, +14.9 m, +16.8 m, +21 m, +23 m and +29.2 m (Figs. 5 and 6). In addition to the production building and the pools of ISFSI building № 1 of MCP 186, which was digitized on a timeline of 20 sec, the three-component 39-axis floor accelerograms were obtained at elevation marks of +5.5 m, +6 m, +8.55 m, +11.3 m, +12.05 m and +15.1 m (Fig. 7).

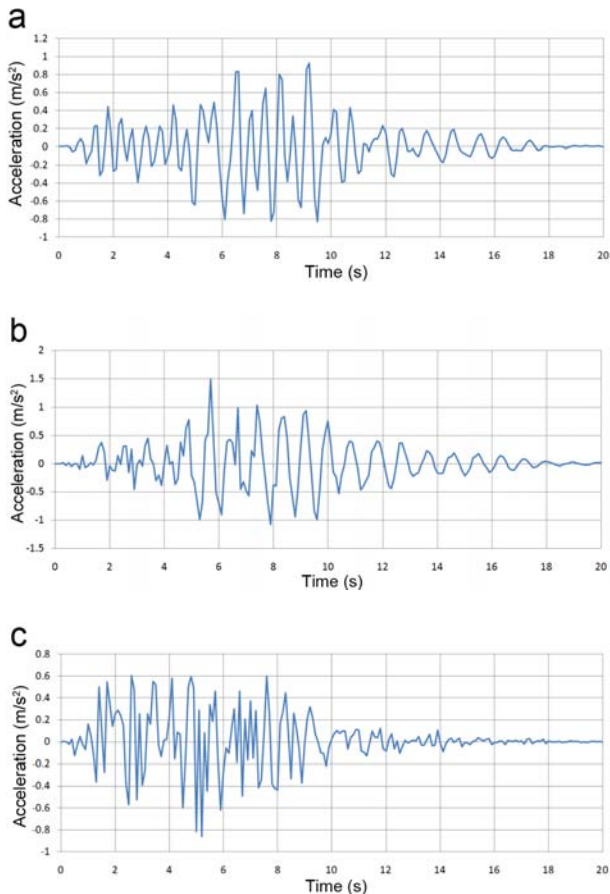


Fig. 5- Three-component floor accelerogram of the receiving department of ISFSI building № 1 of MCP at an elevation mark of +23 m on the runway rails of the 160/32-ton crane (node № 351, see Fig. 3b): a and b – the X and Y horizontal components; c – the Z vertical component

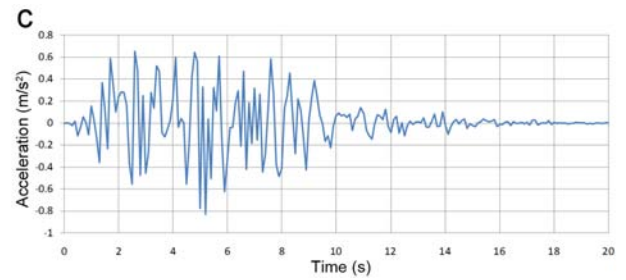
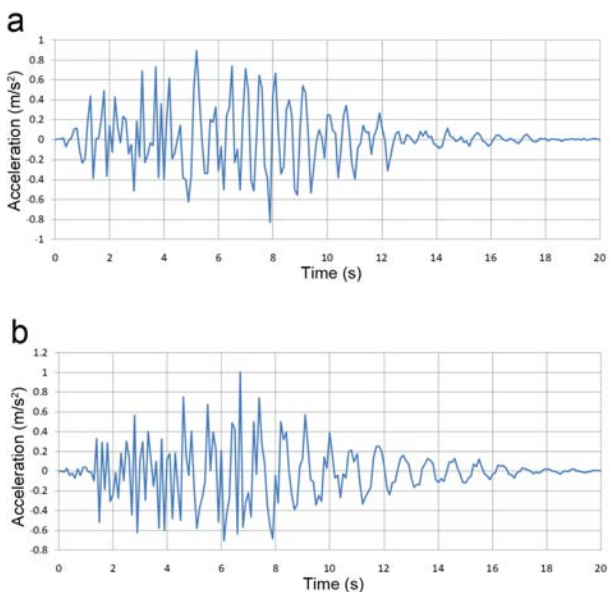


Fig. 6-Three-component floor accelerogram of the receiving department of ISFSI building № 1 of MCP at an elevation mark of +16.8 m on the runway rails of the 16/3.2-ton crane (node № 340, see Fig. 3b): a and b - the horizontal X and Y components; c - the vertical Z component

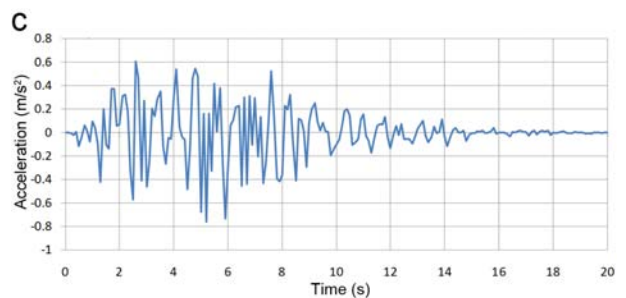
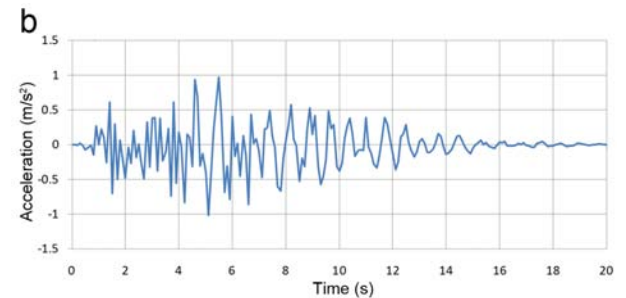
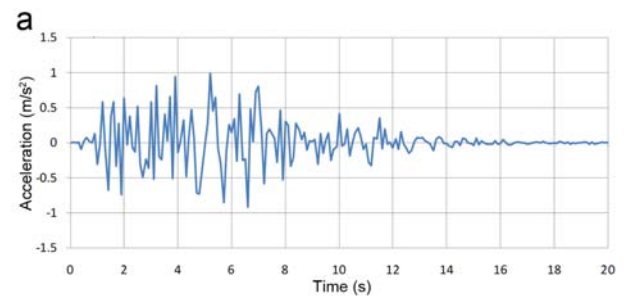


Fig. 7-Three-component floor accelerogram of the production building and the pools of ISFSI building № 1 of MCP at an elevation mark of +8.55 m on the runway rails of the 15-ton crane (node № 291, see Fig. 4b): a and b - the horizontal X and Y components; c - the vertical Z component

## 4 Dynamic Models of the Cranes of the ISFSI Building

As illustrated in Fig. 8, the dynamic model of the 160/32-ton crane, which is loaded by a traverse and a container TC-13, has  $n=3486$  degrees of freedom and consists of 863 FEs, which include 762 beams, 90 shells, 11 cable FEs and 581 nodes. The working drawings of the bridge cranes (№ 1, registration number № 11-003, load capacity (LC) 160/32 tons; № 2, registration number № 11-004, LC 16/3.2 tons; № 3, registration number № 11-005 and № 4, registration number № 11-006, LC 15 tons) and the working drawings of the design of containers TC-10 and TC-13, the cases, the fuel assemblies (FA) of the VVER-1000 reactor, the traverses for TC-10 and TC-13, the bars and the extension bars [13] were the basic data to develop a dynamic model of the technical systems of the crane equipment and the technological loose gear of ISFSI under the service load combination and the floor seismic loads.

Similarly, the dynamic model of crane № 2 with an LC of 16/3.2 tons, which is loaded by bar "B" and case 02HM with FA, has  $n=3426$  degrees of freedom and consists of 847 FEs, which include 668 beams, 172 shells, 7 cable FEs and 571 nodes.

The dynamic model of crane № 3, registration number № 11-005 and crane № 4, registration number № 11-006, with an LC of 15 tons, which are loaded by bars "A" and cases 02HM with FA, has  $n=8310$  degrees of freedom and consists of 1824 FEs, which include 1212 beams, 606 shells, 6 cable FEs and 1385 nodes.

## 5 Mathematical Model of the Probability-Statistical Floor Accelerograms

To calculate the seismic stability of the crane systems as an input seismic action (SA), the floor probability-statistic accelerograms were used. These accelerograms were calculated using the floor accelerograms of a building with independent spent fuel storage installation (ISFSI) depending on the installment position of the crane runway rails and their elevation marks. The probabilistic models of SA are the statistical average and the probability-statistical floor accelerograms (SAFA and PSFA), which are plotted based on an ensemble of floor accelerograms of the receiving department, the production building and the pools of ISFSI building № 1 of MCP; the accelerograms correspond to the same elevation marks of +23 m, +16.8 m and 8.55 m at the installment level of crane runway rails. To

plot SAFA and PSFA, the authors accepted the following assumptions [14, 15]: 1) during the action time  $\tau_e$  of the effective phase of an earthquake,  $4s \leq \tau_e \leq 20$  s, SA is a stationary random process with zero mathematical expectation, variance  $\sigma_a^2$ , correlation function (CF)  $K(\tau)$  and spectral density function (SDF)  $G_a(\omega)$ ; 2) the seismic action, which is specified by the accelerogram  $a(t)$ , has a normal distribution with the following probability density function:

$$f(a) = \frac{1}{\sigma_a \sqrt{2\pi}} \exp\left(-\frac{(a - \langle a \rangle)^2}{2\sigma_a^2}\right); \quad (11)$$

3) SA is set for three spatial directions: two horizontal X and Y directions and one vertical Z direction, where the probability of a design-basis earthquake (DBE) is equal to  $T_{CR}/10^2$  and MCE is equal to  $T_{CR}/10^4$ . The quantity  $T_{CR}$  is the normative service life of a crane, which is taken (a) mediately depending on the number of stress cycles of the crane's metal constructions and mechanisms according to ISO 4301/1, (b) depending on the importance class of the crane according to GOST 28609-90 "Load lifting cranes. Principal provisions of calculation", (c) for general purpose cranes according to RD 10-112-1-04[16] and (d) for cranes of FUNE considering the requirements of NP 043-03 [5].

We will represent SA as a random function  $\tilde{a}(t)$  by ensemble of choice functions  $\{a_i(t)\}$ , none of which describes all characteristics of SA. After staticizing the ensemble of the initial floor accelerograms (see Figs. 5-7), we will obtain the action that considers all characteristics of the ensemble. Thus, each accelerogram of the initial ensemble is redigitized with the same step  $\Delta t$  ( $0.01 \text{ c} \leq \Delta t \leq 0.03 \text{ c}$ ), and for each of them, a duration is set corresponding to duration  $\tau_e$  of the effective phase of the ensemble. As a result, we have an ensemble of accelerograms of equal duration, which have been redigitized with equal time step and are regarded as a realization of the random process  $\tilde{A}(t)$ . For each time point  $t_k$  (with digitization step  $\Delta t$ ), the instantaneous values of the earthquake process are averaged out; i.e., the mathematical expectation  $\langle a | t_k \rangle$  and the mean square value  $\sigma_{a|t_k}^2$  are determined

$$\langle a | t_k \rangle = \sum (a_i | t_k) / S;$$

$$\sigma_{a|t_k}^2 = \sum (a_i | t_k - \langle a | t_k \rangle)^2 / (S - 1), \quad (12)$$



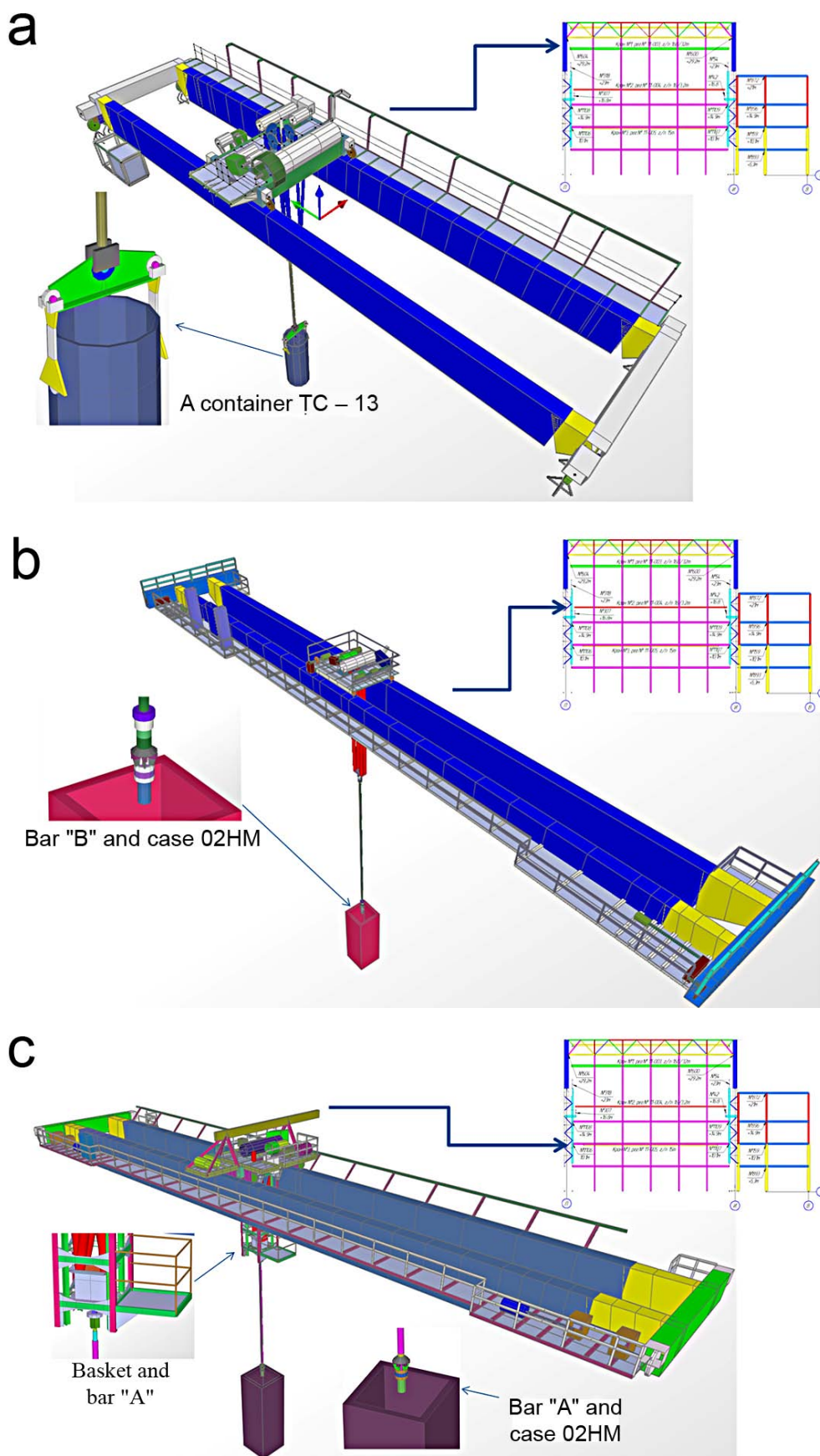


Fig. 8- Dynamic models: a- crane № 1, reg. № 11-003, LC 160/32 t; b-crane № 2, reg. № 11-004, LC 16/3.2 t; c- crane № 3, reg. № 11-005, and crane № 4, reg. № 11-006, LC 15 t

where  $S$  is the number of realizations of the calculated floor seismic processes.

The sample of  $a_i | t_k$  of size  $S$  in (11) and (12) has the normal distribution (11). By changing the sample size, its mathematical expectation and variance (12) will change. On this occasion, for the time point  $t_k$ , the value of the process  $\langle a | t_k \rangle$  is a random variable with its own parameters of variance

$$\sigma_{\langle a | t_k \rangle} = \sigma_{a | t_k} / \sqrt{S} \quad (13)$$

and mathematical expectation of the sample mean, whose probability  $P = F(U_p) = 2\Phi(U_p)$  is in the interval

$$\begin{aligned} (\langle a | t_k \rangle - U_p \sigma_{a | t_k} / \sqrt{S}) \leq \mu \leq \\ \leq (\langle a | t_k \rangle + U_p \sigma_{a | t_k} / \sqrt{S}) \end{aligned}, \quad (14)$$

where the upper bound in (14) is SAFA:

$$\langle a \rangle_k = \langle a | t_k \rangle + U_p \sigma_{\langle a | t_k \rangle}. \quad (15)$$

In (14) and (15),  $F(U_p)$  and  $\Phi(U_p)$  are tabulated functions of normal distribution (normalized distribution and Laplace distribution);  $U_p$  is a quantile of normal distribution that corresponds to the assumed confidence probability  $P$  [17]. The quantile of Student's distribution  $q_p$  should be taken with a small number of realizations of the seismic process instead of the quantile  $U_p$  in (14) and (15).

The analysis of the floor accelerograms [9] shows that the peak accelerations at the time point  $t_k$  of SAFA, which were built for different ensembles, may substantially differ from each other. Thus, to improve the accuracy of the SA presentation and the quality of the seismic calculations of the cranes, the authors use PSFA. Considering that the mean square value  $\sigma_{a | t_k}$  in (14) is also a random variable with confidence interval

$$(1 - q_p) \sigma_{a | t_k} \leq \sigma_{a | t_k} \leq (1 + q_p) \sigma_{a | t_k}, \quad (16)$$

where  $q_p$  is a quantile of distribution and in plotting PSFA, it is reasonable to obtain the upper bound of the  $P$ -percentage interval of the root mean square value of  $\sigma_{a | t_k}$  from (16). Afterwards, PSFA has the form

$$a_k = [\langle a_k | t_k \rangle + U_p \sigma_{\langle a | t_k \rangle}] + U_p \sigma_{a | t_k} (1 + q_p), \quad (17)$$

which considers the  $P$ -percentage of properties of the entire initial information of the ensemble  $\{a_i(t)\}$ , and PSFA can be used as a model of SA in the calculations of the crane seismic stability using the linear-spectral method (LSM) or DAM. It is obvious that PSFA (17) 7, 8 and 9b on the MSK-64 scale should be recommended to use for the practical calculations of the cranes under SA by DAM, and the choice of values of the confidence probability  $P$  in (17) depends on the probability

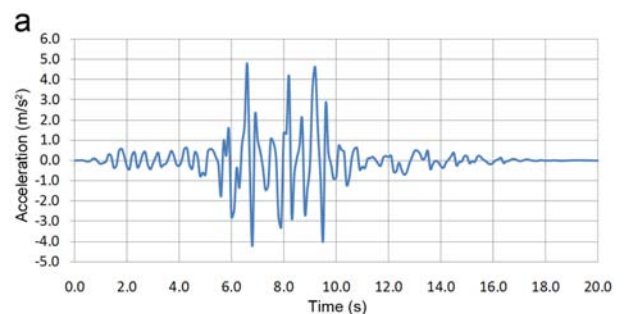
$$\alpha = 1 - P, \quad (18)$$

which is called the risk of the 1st kind and determines the range in which an  $\alpha$  percentage of the probable unaccounted average sample estimates falls. For the practical calculations of the cranes under SA, to obtain the digitalization values of the accelerogram  $a(t)$  with any time step within the limits of the half-cycle length, the following formula is used

$$a(t + \tau) = a_m \sin(\pi\tau/L), \quad (19)$$

where  $L$  is the pulse duration,  $t$  is the pulse start time,  $\tau$  is the time within a pulse,  $0 \leq \tau < L$ , and  $a_m$  is the pulse amplitude.

Using (17), PSFA was plotted for the high elevation marks of the installment of bridge cranes № 1 (reg. № 11-003, LC 160/32 t) (Fig. 9), № 2 (reg. № 11-004, LC 16/3.2 t) (Fig. 10), № 3 (reg. № 11-005) and № 4 (reg. № 11-006, LC 15 t) (Fig. 11). It should be noted that all three-component accelerograms that were mentioned in this study were digitized as a process on a time line with time step  $\Delta t$ , ( $0.01 \text{ s} \leq \Delta t \leq 0.03 \text{ s}$ ). On average, the ISFSI building amplifies the horizontal components of SA in 1.4 times and damps the vertical component in 1.25 times, as observed from the analysis of the initial floor accelerograms (see Figs. 5-7) and PSFA (see Figs. 9-11).



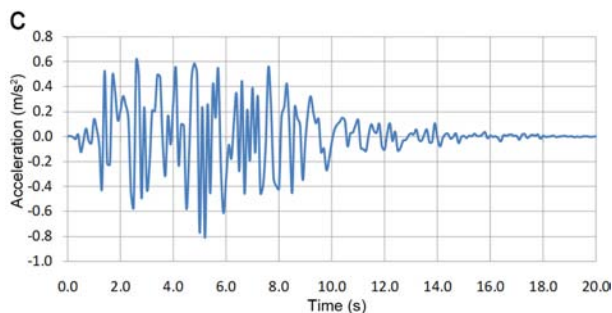
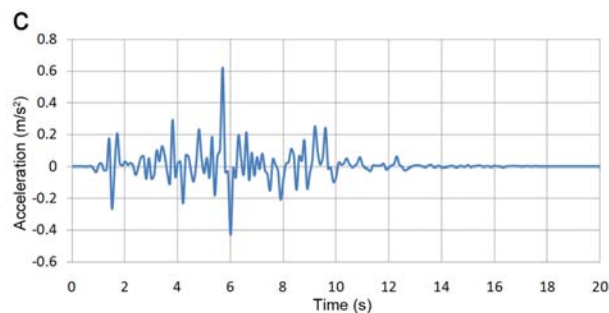
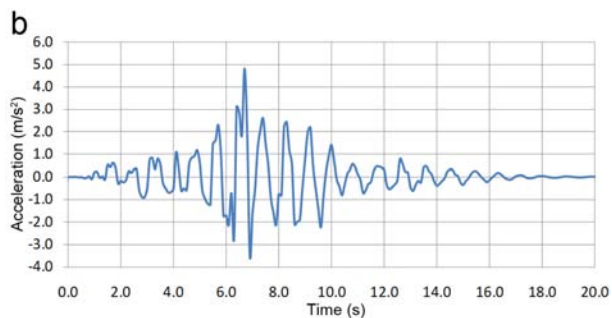


Fig. 10- Probability-statistical floor three-component accelerogram at installment elevation mark +16.8 m of the runway rails of bridge crane № 2 (reg. № 11-004, LC 16/3.2 t) in the receiving department of ISFSI building № 1 of MCP: a and b - horizontal X and Y components; c - vertical Z component

Fig. 9- Probability-statistical floor three-component accelerogram at installment elevation mark +23 m of the runway rails of bridge crane № 1 (reg. № 11-003, LC 160/32 t) in the receiving department of ISFSI building № 1 of MCP: a and b - horizontal X and Y components; c – vertical Z component

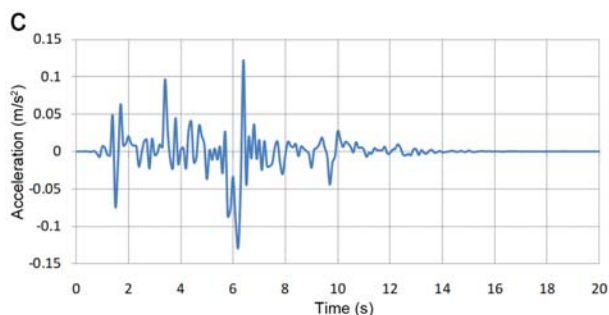
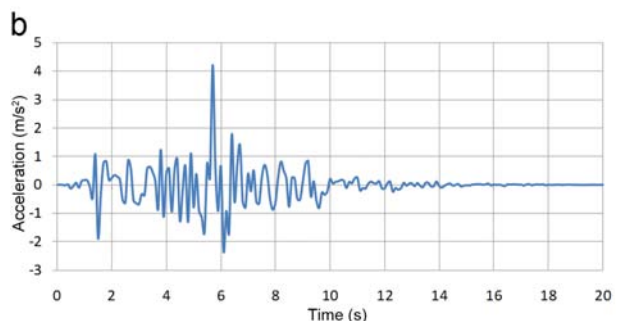
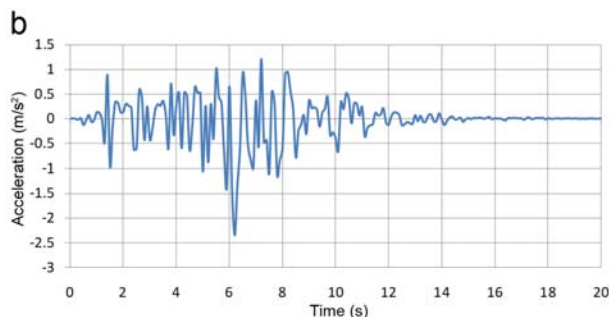
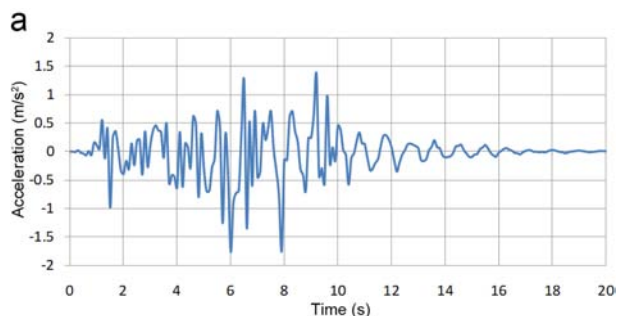
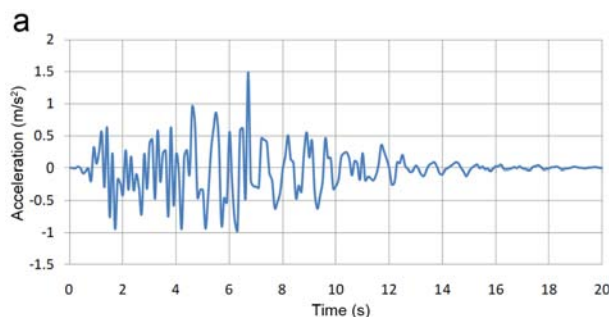


Fig. 11- Probability-statistical floor three-component accelerogram at installment elevation mark +8.55 m of the runway rails of bridge crane № 3 (reg. № 11-005) and crane № 4 (reg. № 11-006, LC15T) in the building with the spent-fuel pools: a and b -horizontal X and Y components; c - vertical Z component

### 6 Mathematical Model of the Seismic Response Spectra

The response spectra (SRS) represent a relation between the maximum accelerations of oscillators  $A(t) = \max \ddot{x}(t)$  and their natural frequency (NF)  $\omega_m$  (from 1 to 30 Hz) at various damping values  $\zeta$  of the metal construction of the cranes. SRS are the result of the action of a given accelerogram  $a(t)$  (real, synthesized, for example, SA-482[3], or PSFA, which was calculated using formula (17)). When SRS were given to the designer to estimate the seismic safety of the load-lifting cranes, such approach do not contradict clause 2.1.6 PB 10-382-00 [18] and SNiP II-7-81\* [1]. However, if there is no SRS and they should be plotted as floor SRS (FSRS), then PSFA must be transformed to the standard levels (Table 2) [19].

Table 2. Maximum level of calculated accelerations of earthquakes [19].

Seismicity, the values are on the MSK-64 scale	5	6	7	8	9	10
Maximum level of accelerations (m/s <sup>2</sup> )	0.25	0.5	1	2	4	8

Therefore, to obtain the FSRS floor accelerograms  $A_0(\tau)$  (see Figs. 9-11), we must numerically integrate the equation of motion of the  $m$ th oscillator:

$$\ddot{x}(t) + 2\zeta\dot{x}(t) + \omega_m^2 x(t) = -A_0(t), \quad (20)$$

where  $\zeta$  is the relative damping of the crane metal construction coefficient ( $\zeta=0.02-0.04$ ), which is associated with the logarithmic decrement of oscillations of the dynamic model of crane  $\delta_d$  by the following relationship [8,9,14]:

$$\zeta = \delta_d / (2\pi) \approx \delta_d / 2\pi. \quad (21)$$

Afterward, from the solution of (20), the maximum value of reaction  $\max(\ddot{x}(t))_m$  is chosen, which is considered the response of the oscillator of medium frequency (MF)  $\omega_m$ . Given zero initial conditions, instead of equation (20), the Duhamel integral [20] is recommended:

$$x(t) = (1/m\omega_{mD}) \int_0^t a(\tau) \exp[-\zeta\omega_{mD}(t-\tau)] \times \sin \omega_{mD}(t-\tau) d\tau, \quad (22)$$

where  $\omega_{mD}$  is the MF of the  $m$ th oscillator, which is corrected considering damping (21):

$$\omega_{mD} = \sqrt{\omega_m^2 - \zeta^2}. \quad (23)$$

Obviously, the three-component SRS and FSRS are plotted with the frequency axis up to 30 (rarely 50) Hz as a rule, where for each  $\omega_m$ , a sampling corresponds from (20) or from (22) (Figs. 12 and 13); from the three-component SRS and FSRS, we can transition to the seismic amplification factors (SAF) of SNiP II-7-81\*[1] or RTM 108.020.37-81 [19] according to [21] if necessary.

In addition to the real SRS or FSRS, the generalized seismic response spectra (GSRS) are of practical concern. GSRS are spectra that were obtained as an envelope of assemblage of SRS for a set of real and/or synthesized accelerograms of earthquakes [21]. As consistent with the principal provisions of theory of the seismic stability of buildings [1, 3, 22], where the fundamental is LSM, it should be considered that the seismic amplification factors (SAF) [1] were set for building structures with logarithmic decrements of oscillation damping  $\delta_d = 0.4$ , whereas  $\delta_d$  of the metal constructions of the lifting equipment [23] do not exceed  $\delta_d = 0.2$  even under MCE [13]. Thus, the algorithm of the plane problem of LSM of SNiP II-7-81\* [1] does not make it possible to study a spatial work of beam systems of cranes under the conditions of SA. In this connection, the authors of this study attempt to develop the LSM of the theory of seismic stability of the spatial constructions of load-lifting cranes.

The basis of LSM is a conception about the dynamic system of a crane as a collection of independent  $m$ -oscillators, the vibration frequencies  $\omega_m$  of which coincide with the natural frequency spectrum of the calculated system of a crane. Then, the reaction of the system to SA is determined as a sum of the maximum reactions of the oscillators that compose the system. Examine the forced seismic oscillations of an undamped system (a dynamic model of a crane) with  $n$  degrees of freedom:

$$[M]\{\ddot{V}(t)\} + [K]\{V(t)\} = -[M]\{\ddot{A}(t)\}, \quad (24)$$

where  $[M]$  and  $[K]$  are the mass matrix and the stiffness matrix of the dynamic model of the crane construction, respectively (see part 1 of the article). In the matrix equation (24),  $\{\ddot{A}(t)\}$  is the SA vector, which is set by PSFA (see Figs. 9-11).

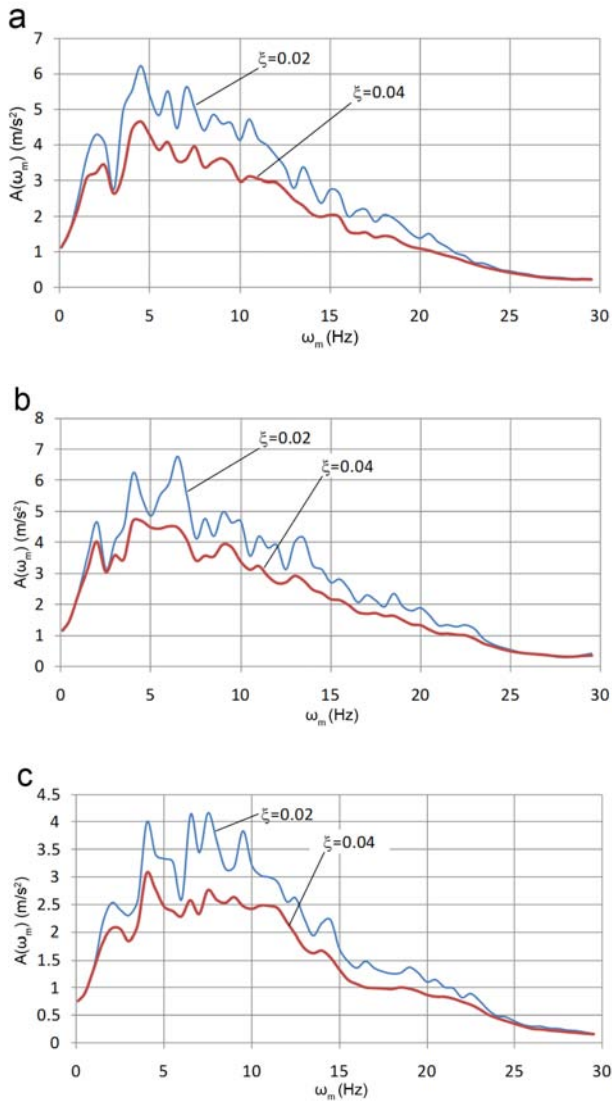


Fig. 12- SRS obtained for the synthetic three-component accelerogram of MCE of magnitude 7.0 at  $\xi=0.02$  and  $\xi=0.04$ : a, b – horizontal components, c – vertical component.

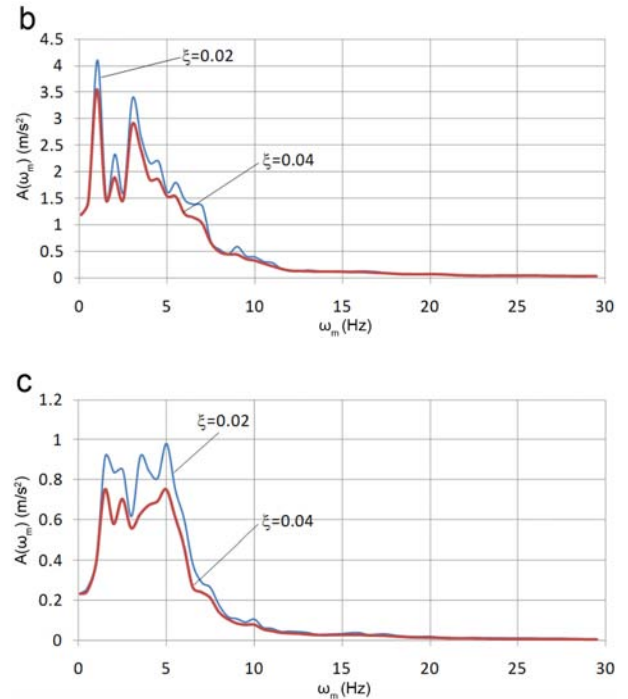
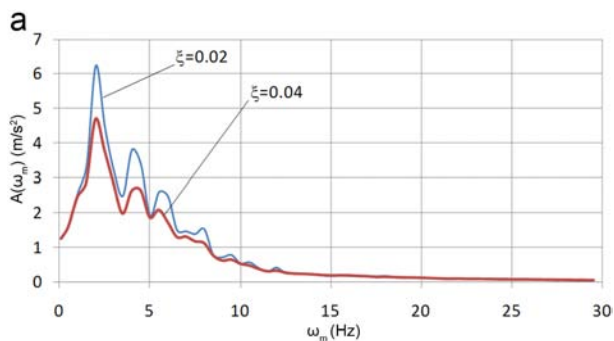


Fig. 13- FRS calculated for the three-component floor accelerogram of the receiving department of ISFSI building № 1 of MCP at elevation mark +23 m of the runway rails of the crane with LC 160/32 t at  $\xi=0.02$  and  $\xi=0.04$ : a, b – horizontal components, c – vertical component.

The damping in (21) can be considered after the transition to normal coordinates when the respective floor seismic response spectrum (FRS) is used. Then, as a new basis, we will take eigenvectors that were obtained for the current dynamic system from the equations of free oscillations (25), which were obtained from (24).

$$[M]\{\ddot{V}(t)\} + [K]\{V(t)\} = \{0\}, \quad (25)$$

The connection between the generalized coordinates  $\{V\}$  and the normal coordinates  $\{\psi\}$  is determined by a relation:

$$\{V\} = [\Phi]\{\psi\}, \quad (26)$$

where the matrix  $[\Phi]$  contains eigenvectors (mode shapes)  $\{\phi_i\}$  as columns, which are determined from the matrix equation for eigenvalues

$$([K] - [\Lambda][M])[ \Phi ] = \{0\}.$$

Here

$$[\Lambda] = \begin{bmatrix} \omega_1^2 & \omega_2^2 & \dots & \omega_m^2 & \dots & \omega_n^2 \end{bmatrix},$$

is the squared natural frequencies of the dynamic model of the crane diagonal matrix.

Substitute (26) and its second derivative into (24), then multiply the obtained equation by the transposed vector of the  $m$ th mode shape:

$$\{\phi_m\}^T [M][\Phi]\{\ddot{\psi}\} + \{\phi_m\}^T [K][\Phi]\{\psi\} = -\{\phi_m\}^T [M]\{\ddot{A}(t)\} \quad (27)$$

According to the orthogonality condition, which was proved by Rayleigh, equation (27) takes the form:

$$M_m \ddot{\psi} + K_m \psi = -\{\phi_m\}^T [M]\{\ddot{A}(t)\}, \quad (28)$$

where  $M_m$  and  $K_m$  are the modal mass and the stiffness, respectively:

$$M_m = \{\phi_m\}^T [M]\{\phi_m\}; K_m = \{\phi_m\}^T [K]\{\phi_m\}. \quad (29)$$

## 7 Development of the LSM Theory

The vector in the right part of (28) may be interpreted as a portion of the seismic load on the crane that causes the oscillations of the dynamic model of the crane in the  $m$ th shape. If we present SA in (28) as

$$\{\ddot{A}(t)\} = \{\overline{\cos}\} \ddot{A}_0(t), \quad (30)$$

where  $\{\overline{\cos}\}$  is the vector of direction cosines of the components of the accelerogram in GCS and equation (28), considering damping, (21) has the form:

$$\ddot{\psi} + 2\xi_m \omega_m \dot{\psi} + \omega_m^2 \psi = -D_m \ddot{A}_0(t), \quad (31)$$

where  $\omega_m$  is the natural oscillation frequency of the oscillator:  $\omega_m^2 = K_m/M_m$ ,  $\xi_m$  is the damping ratio according to (31),  $D_m = \{\phi_m\}^T [M]\{\overline{\cos}\}/M_m$  is the influence coefficient, which is constant for the  $m$ th mode shape. Introduce a new independent variable  $y$  such that

$$\psi = D_m y, \quad (32)$$

then equation (31) can be written in the form of the equation of motion of an oscillator with a single mass that executes forced oscillations under a

seismic load, and the load is set by the accelerogram of an earthquake  $\ddot{A}_0(t)$  from (30):

$$\ddot{y} + 2\xi_m \omega_m \dot{y} + \omega_m^2 y = -\ddot{A}_0(t). \quad (33)$$

From (24), (28) and (33), it follows that the seismic loads are unknown inertial loads, and to determine their values, it is necessary to obtain the absolute accelerations of the earth. For the multi-mass systems of load-lifting cranes, the seismic loads are determined by the following vector:

$$\{S(t)\} = [M]\{\ddot{V}_a(t)\}, \quad (34)$$

where  $\{\ddot{V}_a(t)\}$  is the vector of absolute accelerations of the earth in generalized coordinates.

Considering (28) and (34), the contribution from the  $m$ -th shape mode of the crane construction to the calculated seismic load can be presented in the form

$$\{S(t)\}_m = [M]\{\phi_m\} D_m \ddot{y}_{a,m}(t). \quad (35)$$

Here,  $\ddot{y}_{a,m}(t)$  is the absolute acceleration of the  $m$ -th oscillator under SA  $\ddot{A}_0(t)$ . In the LSM of the spatial constructions of the lifting equipment, a transition from dynamic problem (35) to a quasi-static problem is fundamentally important. It is implemented by replacing the time function  $\ddot{y}_{a,m}(t)$  in (35) with the constant quantity  $\ddot{y}_{a,m}$ , which represents the maximum response of the oscillator with frequency  $\omega_m$  to the action that is set by the accelerogram  $\ddot{A}_0(t)$  (see (20)). The quantity  $\ddot{y}_{a,m}(t)$  in (35) should be obtained from FSRS for any given accelerogram (see Figs. 9-11). Therefore, the  $m$ th seismic force in accordance with LSM can be calculated using the response spectra (FSRS) as follows:

$$\{S\}_m = [M]\{\phi_m\} D_m W(\omega_m, \xi_m), \quad (36)$$

where  $W(\omega_m, \xi_m)$  is a value of the seismic response spectrum with damping  $\xi_m$  on frequency  $\omega_m$ , and it is plotted for the floor accelerogram  $\ddot{A}_0(t)$ . In addition,  $\ddot{y}_{a,m} = W(\omega_m, \xi_m)$ .

If the source accelerogram (PSFA) is specified by the three-component action of the form (30), which occurs most often in practice, then the seismic load in the  $m$ -th mode shape on the crane construction can be calculated using the following formula:

$$\{S\}_m = [M] \{\phi_m\} \frac{\{\phi_m\}^T [M]}{\{\phi_m\}^T [M] \{\phi_m\}} \{W(\omega_m, \xi_m)\}, \quad (37)$$

where  $\{W(\phi_m, \xi_m)\}$  is the vector of the  $n^*$  order that was plotted based on the three-component FSRS using PSFA(27). In addition,  $n^* < n$ , where  $n$  is the number of degrees of freedom of the dynamic model of the crane (lifting equipment), and  $n^* = 30 \div 50$  Hz, where:

$$\{W(\phi_m, \xi_m)\} = \left\{ \begin{array}{l} \{W_x(\phi_m, \xi_m), W_y(\phi_m, \xi_m), W_z(\phi_m, \xi_m), 0, 0, 0, 0\}_1^T \\ \dots \\ \{W_x(\phi_m, \xi_m), W_y(\phi_m, \xi_m), W_z(\phi_m, \xi_m), 0, 0, 0, 0\}_n^T \end{array} \right\}. \quad (38)$$

In fact, in the scope of LSM, a concept of quasi-static seismic forces  $\{S\}_m$  (27) is introduced. Each force along the  $m$ -th mode shape of the dynamic model of the crane is characterized as follows: if we apply an equivalent vector of static forces, then the metal construction of the crane will obtain seismic displacements  $\{V\}_m$  that are determined from the condition of static equilibrium:

$$[K] \{V\}_m = \{S\}_m. \quad (39)$$

Using the obtained vector of displacements from (24), according to FEM, the unknown vector of internal forces  $\{Q\}_m$  in each  $jk$  FE of the dynamic model of the crane construction is determined in GCS:

$$\{Q\}_m^{jk} = [k]_{oxyz}^{jk} [T]_{14 \times 14} \{v\}_m^{jk}, \quad (40)$$

where  $[T]_{14 \times 14}$  is the «LCS→GCS» transformation matrix [23],  $[k]_{oxyz}^{jk}$  is a  $14 \times 14$  stiffness matrix of thin-walled  $jk$  FE, and  $\{v\}_m^{jk}$  is a 14<sup>th</sup>-order vector of displacements of nodes  $j$  and  $k$  of  $jk$  FE, which is obtained from the  $n$ th-order vector  $\{V\}_m$  that was obtained in the result of solution (39):

$$\{v\}_m^{jk} = \left\{ \begin{array}{l} \left( \delta_x \delta_y \delta_z \varphi_x \varphi_y \Theta_z \Theta'_z \right)^{T,j} \\ \left( \delta_x \delta_y \delta_z \varphi_x \varphi_y \Theta_z \Theta'_z \right)^{T,k} \end{array} \right\},$$

where each row contains the linear displacements of the  $j(k)$  node along the XYZ axes of GCS, the three

angular displacements and a derivative of the twist angle ( $\Theta'_z$ ).

As a rule, the resultant internal forces (40) from the action of the calculated seismic forces (37) must be obtained by summing the vectors (40) for all accounted  $n^*$  mode shapes up to 30 Hz. However, because their values for different natural modes are obtained in different points of time, they cannot be obtained using LSM. Therefore, a total calculated internal force (40) is determined using the empirical formulas (which were ascertained by comparing the calculation by LSM and the dynamic analysis method (DAM) with an input action that was set by the accelerogram) with a root-mean-square summation in particular:

$$\{Q\}_s = \sqrt{\sum_{m=1}^{n^*} (\{Q\}_m)^2}, \quad (41)$$

where  $n^* \ll n$  is the number of accounted mode shapes. For closely spaced natural frequencies of the dynamic model of cranes such that  $\omega_i \leq 1.1\omega_{i-1}$ , the internal forces (40) that are obtained using the root-mean-square summation method (41) are smaller than the internal forces that are obtained using DAM. In this case, the authors [24, 25] recommend using algebraic summation in groups and root-mean-square summation for the obtained sums:

$$\{Q\}_s = \sqrt{\sum_{m=1}^q \left( \sum_{l=1}^{r_q} |\{Q\}_{m,l}| \right)^2}, \quad (42)$$

where  $q$  is the number of groups;  $r_q$  is the number of frequencies in the  $q$ th group. The internal forces (42), which were obtained using root-mean-square summation, do not have signs; thus, their directions are unknown. Therefore, under LSM, the worst acceptable loading conditions are obtained when the static operating load directions and the calculated seismic load directions coincide. Hence, the total internal forces for each  $jk$  FE are evaluated using the following formula:

$$\{Q\} = \{Q\}_e + \text{sign}(\{Q\}_e) \cdot \{Q\}_s. \quad (43)$$

## 8 Equation of the Seismic Oscillations on the DAM Basis

The proposed development of the theory of LSM enables one to make calculated analysis of the seismic safety of spatial metal constructions of

cranes. However, the proposed methodology overrates the internal forces (43) by 20-25% on average and consequently overrates the specific metal quantity of cranes in the seismic stability of the crane design (according to the requirements of PB 10-382-00 [18]). Thus, the authors of the present study find it necessary to apply a further methodological transition from LSM to the DAM [23] mathematical model, which is a matrix of differential equations of motion of the  $n$ th order of the form

$$[M]\{\ddot{V}(t)\} + [C]\{\dot{V}(t)\} + [K]\{V(t)\} + \{R(\dot{V}(t), V(t))\} = \{R_{ST}\} - [M](\overline{\cos})\ddot{A}(t). \quad (44)$$

Assuming that the reader is familiar with the nonlinear equation of seismic oscillations of the spatial constructions of cranes (44), we should dwell on two factors. The first factor is associated with the formulation of the damping matrix. In the linear equations of motion (44) (for  $\{R(V, \dot{V})\} = 0$ ), the recommended form of the damping matrix is proportional to the mass matrix and the stiffness matrix of the calculated system:

$$[C] = \alpha_{[M]}[M] + \alpha_{[K]}[K], \quad (45)$$

where the constants of proportionality

$$\alpha_{[M]} = (\delta_{d,1}\omega_1) / \pi; \quad \alpha_{[K]} = \delta_{d,1} / \pi\omega_1,$$

depend on the decrement  $\delta_{d,1}$  (see formula (21)) and the frequency  $\omega_1$  of the lowest natural mode shape of the construction elements of the crane dynamic model. The recommendations to determine  $\delta_{d,1}$  may be found in [23, 24, 26]. Moreover, (45) is used extensively in the computational practice damping matrix with frequency-independent internal friction of A. I. Tseitlin [27]:

$$[C] = [M]([M]^{-1}[K])^{0.5} [G], \quad (46)$$

where  $[G]$  is the (damped) loss matrix. For homogeneous constructions such as the sheet-welded metal constructions of bridge cranes

$$[G] = \gamma_d = \delta_d / \pi. \quad (47)$$

Along with (37),

$$\gamma_d = 4\gamma / 4 - \gamma^2, \quad (48)$$

where  $\gamma$  is the coefficient of internal friction of Sorokin E.S. [28]. From (48), one can see that  $\gamma_d \approx \gamma$ ; thus, matrix (46) is transformed to the less popular damping matrix of V.T. Rasskazovski and A.I. Martemjanov [29]

$$[C] = \gamma_d ([M][K])^{0.5}. \quad (49)$$

The second factor concerns the determination of the node internal forces in the end sections of the finite elements of the crane dynamic model after solving the matrix equation (44) and calculating the vector of unknown displacements  $\{V(t)_{1 \times n}\}$  in the general coordinate system  $oxyz$ .

## 9 Seismic Safety Criterion of the Load-Lifting Cranes in Buildings with Crane Loadings

The known vector of internal forces at the ends of the  $jk$  element in the local coordinate system  $oxyz$  has the following structure

$$\{Q\}_{14 \times 1}^{jk} = \left\{ \begin{array}{l} (Q_x Q_y N_z M_x M_y M_z B)_j^T \\ (Q_x Q_y N_z M_x M_y M_z B)_k^T \end{array} \right\}, \quad (50)$$

and it is a result of shear deformation, tension-compression, bending, torsion and deplanation, where  $B$  is the bimoment known from the theory of thin-walled bars of Vlasov and Umanski [30]. If  $\{V(t)\}_{oxyz}^{jk}$  are the node displacements of the  $jk$  finite element in the general coordinate system, then its node internal forces  $\{Q(t)\}_{oxyz}^{jk}$  in the local coordinate system  $oxyz$  will be calculated from the following equation

$$\{Q(t)\}_{oxyz}^{jk} = [K]_{jk 14 \times 14}^{oxyz} ([T]_{14 \times 14} \{V(t)\}_{oxyz}^{jk}) + \{R_p\}_{oxyz}^{jk}, \quad (51)$$

where  $[K]_{jk 14 \times 14}^{oxyz}$  is the deformational stiffness matrix of the  $jk$  finite element in the local coordinate system  $oxyz$ ,  $\{R_p\}_{oxyz}^{jk}$  is the summation vector of the



reaction external actions, and  $[T]_{14 \times 14}$  is the transformation matrix as mentioned in (51) [31].

As an example, in Fig. 14, a location of the finite elements of crane № 1 with LC 160/32 t (see part 1 of the article) is presented equivalent stresses. According to the 3<sup>rd</sup> theory of failure, the stresses in any point of the section are

$$\sigma_e^{j(k)} = \sqrt{(\sigma^{j(k)})^2 + 4(\tau^{j(k)})^2}. \quad (52)$$

These stress values are close to the yield limit of the basic material of the crane's metal construction. The state of stress of each  $jk$  FE of the crane dynamic model is calculated according to the stresses that occur in its  $j$  and  $k$  end sections from the action of the internal forces (50), which are calculated by integrating equation (44).

Considering (52), the normal stress at any point of the end section  $j(k)$  of the thin-walled  $jk$  FE with an account of deplanation is determined using the following formula:

$$\sigma^{j(k)} = \frac{N_z^{j(k)}}{A} - \frac{M_x^{j(k)}}{I_x} y + \frac{M_y^{j(k)}}{I_y} x + \frac{B^{j(k)}}{I_\omega} \omega_c, \quad (53)$$

where  $x$  and  $y$  are the translational axes of specified points of the section,  $\omega_c$  is the sectorial coordinate, and  $I_\omega$  is the sectorial moment of inertia of the cross section. The shearing stresses in (52) at any point of the end section  $j(k)$  of the thin-walled  $jk$  FE of the open profile are determined using the formula [31]:

$$\begin{aligned} \tau^{j(k)} = & \frac{Q_x^{j(k)} S_y^{j(k)}}{2I_y t_n} + \frac{Q_y^{j(k)} S_x^{j(k)}}{I_x t_c} + \\ & + \frac{M_\omega S_\omega^{j(k)}}{I_\omega t_c} + \frac{M_0^{j(k)}}{I_d t_c}, \end{aligned} \quad (54)$$

The shearing stresses in the  $jk$  FE of the closed profile of the box or the circular section is determined using the following formula:

$$\begin{aligned} \tau^{j(k)} = & \frac{Q_x^{j(k)} S_y^{j(k)}}{2I_y t_n} + \frac{Q_y^{j(k)} S_x^{j(k)}}{2I_x t_c} + \\ & + \frac{M_\omega S_\omega^{j(k)}}{I_\omega t_c} + \frac{M_z^{j(k)}}{A_\Omega t_c}, \end{aligned} \quad (55)$$

where  $M_z = M_0 + M_\omega$  is the total torsional moment,  $M_0 = GI_d \theta'$  is the torsional moment,  $M_\omega$  is the flexural-torsional moment,  $\theta'$  is the derivative of the angle of twist,  $A_\Omega$  is the doubled surface area of the box section,  $S_{x(y,\omega)}$  are the static moments of the cut-off area (see Zhuravski formula) in the considered section,  $t_{c(n)}$  is the wall thickness of a section of the thin-walled FE,  $I_{c(n)}$  is the axial moment of inertia of a section of the thin-walled FE,  $S_{x(y)}^{j(k)}$  is the static moment relative to the axis  $O_x$  ( $O_y$ ) of a part of the cross section of the thin-walled FE above the section that passes through the considered point. Considering (52), the strength condition of the crane's metal construction is

$$n_0 = \sigma_{yield} / \sigma_e^{j(k)} \geq [n_{seism}], \quad (56)$$

where  $[n_{seism}] = 1$  is an allowable load factor of the  $jk$  FE for the combination of working and seismic loads. With (56), it should be noted that condition of seismic strength of the crane can also be established according to another criteria or at request of regulations of the branches of machine construction such as for the cranes that establish atomic energy usage [24], metallurgical cranes, cranes of ports and terminals to transfer dangerous cargos, etc.

In conclusion, it should be noted that according to the seismic analysis results of the crane with LC 160/32 t using DAM (see Fig. 14), the observed horizontal displacements of container TC-10 with SNF of 95 t along the axis  $Y(t)$  during the 9<sup>th</sup> second of an earthquake, which is specified by PSFA, are 4 m (see Fig. 15). This result presents a danger of the destruction of the container in case of its collision while unloading TC-10 from the railway car, and equivalent stresses in a traverse reach 250 MPa (Fig. 16). The connection zone of idle girders, end trucks and end truck equalizers was subject to the strongest seismic analysis. Its failure results in the high radioactive danger of dropping the container TC-10 with SNF (see Fig. 15 a,b).

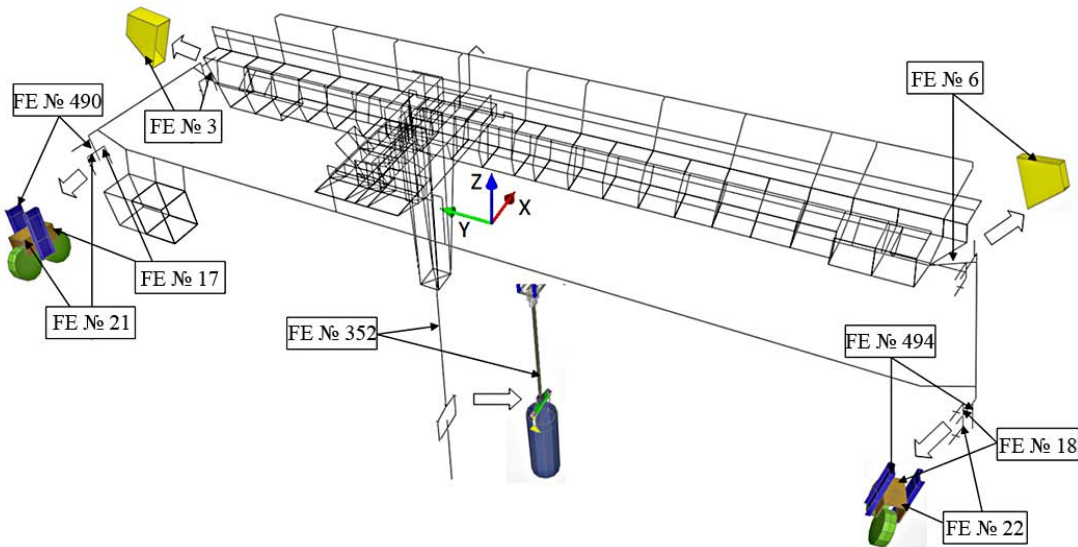


Fig. 14-Location of the most loaded FE of bridge crane № 1 (reg. № 11-003, LC 160/32 t) with the working load "traverse TC-10, container TC-10 with SNF of mass 95 tones" under the seismic action of PSFA

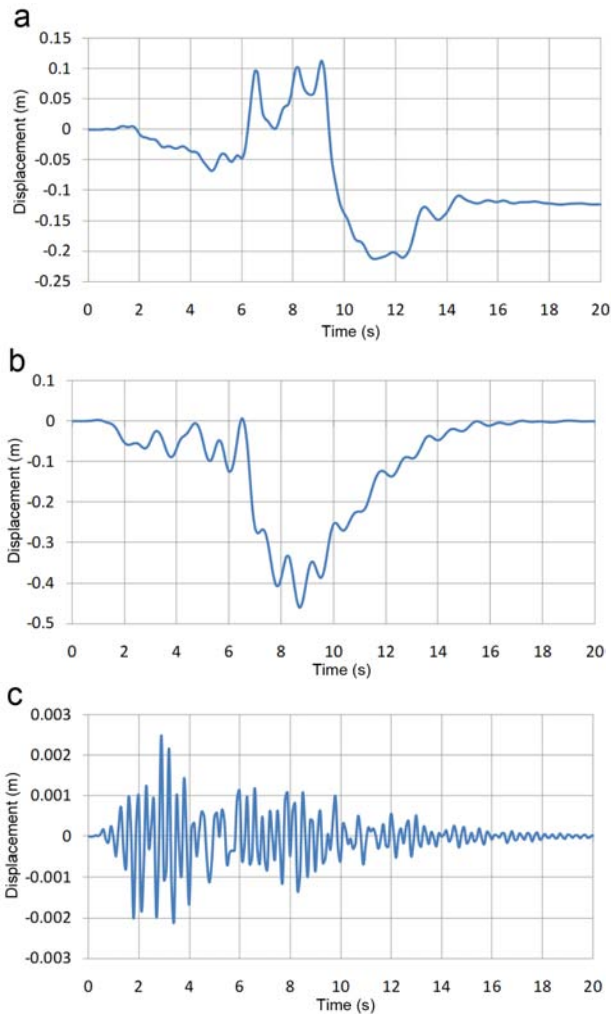


Fig. 15-Displacements of the center of mass of container TC-10 of bridge crane № 1 (reg. № 11-003, LC 160/32 t) under the seismic action of PSFA (see Fig. 9): a - X horizontal, b - Y horizontal, c - Z vertical

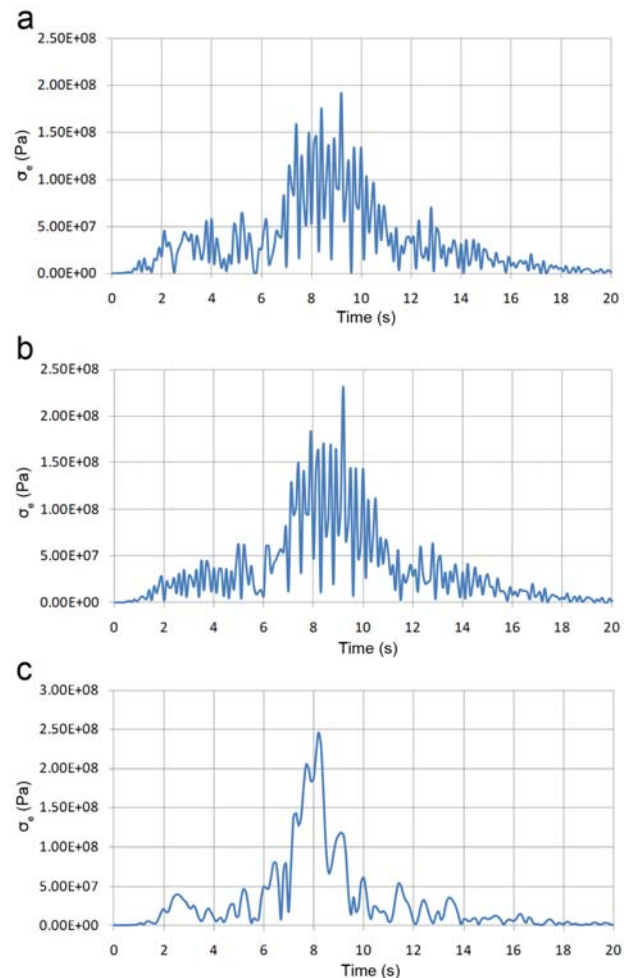


Fig. 16-Equivalent stresses that occur in the FE of crane № 1 (LC 160/32 t) with the working load «traverse TC-10, container TC-10 with SNF of mass 95 tons under the seismic action of PSFA (see Fig. 9): a - FE № 6; b - FE № 21; c - FE № 352 (see Fig. 14)

## 10 Conclusion

The standardization of calculated seismic effects on the industrial buildings of nuclear energy facilities (FUNE) with crane loadings was proposed according to the maps of general seismic regionalization OSR-97.

A discrete-continuum shell-beam dynamic model of the ISFSI building with cranes and crane loadings from cranes with 160/32 t, 16/3.2 t and 15 t was developed based on the FEM principals.

For the dynamic model of the ISFSI building with crane loadings in the 7 magnitude zone, a non-linear equation of the  $n$ th-order seismic oscillations was developed. The equation was solved using the absolutely stable Gear method with the backward differentiation formula. As a result, many calculated floor accelerograms were obtained for the seismic analysis of the subsystems of the ISFSI building and the load-lifting cranes.

For separate levels of the building and zones of crane operation, the calculated probability-statistical floor accelerograms were plotted. The dynamic properties of the ISFSI building was analyzed in the filtration regime of the seismic actions from the ground level to some elevation marks of the ISFSI building.

In accordance with the basic provisions of the theory of seismic stability of structures [1] and the levels of seismic accelerations of 1, 2, 4 and 8 m/s<sup>2</sup> for the 7, 8, 9 and 10 magnitude zones with the damping of the ISFSI building with crane loadings, the floor seismic response spectrum were plotted. The plots are an application by the authors to develop the linear-spectral theory of the spatial shell-beam systems compared to the plane model in [1].

The basics of the theory of seismic stability of the spatial structures of industrial buildings with cranes and crane loadings were proposed based on FEM and DAM by integrating the seismic oscillation equations using the Gear method and the LSM equations of motion, which are solved in principal coordinates by applying the orthogonality conditions of Rayleigh.

The seismic oscillation equations were solved using DAM and LSM for the ISFSI building with crane loadings. The transition from the displacements to the internal forces and then to the normal and tangent stresses was proposed, which is used by the designer to make decisions according to the chosen strength theory.

## References:

- [1] *Construction in Seismic Areas*, SNiP II-7-81\* Standard, 2000 (in Russian).
- [2] *Safety Regulations for Storage and Transportation of Nuclear Fuel at Nuclear Facilities*, NP 061-05 Standard, 2005 (in Russian).
- [3] *Aseismic Nuclear Power Plants Design Code*, NP 031-01 Standard, 2001 (in Russian).
- [4] *Carrying Out of Complex Engineering-Seismic Works at a ISFSI Building №1 Site of the MCP*, Volume 4: *Seismic Zoning and Development of Synthesized Accelerograms According to Soil Characteristics Under Foundation of the ISFSI Building №1*, Moscow: IGE RAS, 2006 (in Russian).
- [5] *Requirements to Arrangement and Safe Operation of Load - Lifting Cranes at Nuclear Power Plants*, NP 043-03 Standard, 2003 (in Russian).
- [6] *General Provisions for Safety of Nuclear Fuel Cycle Plants*, NP 016-05 Standard, 2005 (in Russian).
- [7] *Determination of Initial Seismic Vibrations of Soil for Design Basis*, RB 006-98 Standard, 1998 (in Russian).
- [8] N. Panasenko, *Dynamics and Seismic Stability of Lifting-and-Transport Equipments of Nuclear Power Plants*, Part 1, Ph.D. dissertation, Dept. Load-Lifting Machines, NPI, Novocherkassk, 1992 (in Russian).
- [9] A. Sinelshchikov, *Dynamics and Seismic Stability of Bridge Cranes*, Candidate of Science dissertation, Dept. Load-Lifting Machines, ASTU, Astrakhan, 2000 (in Russian).
- [10] A. Arushanyan, S. Zaletkin, *Numerical Solution of Ordinary Differential Equations Using FORTRAN*, Moscow: MSU, 1990 (in Russian).
- [11] C. Gear, *Numerical Initial Value Problems in Ordinary Differential Equations*, N.J.: Prentice - Hall, 1971.
- [12] V. Myachenkov, *Calculation of Machinery Structures by FEM*, Moscow: Mashinostroenie, 1989 (in Russian).
- [13] N. Panasenko, A. Sinelshchikov, Technical Safety of Shipping Packaging Sets for Spent Nuclear Fuel, *Lifting-and-Transport Equipments (Ukraine)*, Vol.27, №3, 2008, pp. 55-83 (in Russian).
- [14] V. Kotelnikov, N. Panasenko, A. Sinelshchikov, Development of an Earthquake Model for a Calculating Analysis of Seismic

- Stability of Lifting Structures, *Work Safety in Industry*, №9, 2007, pp. 42-46 (in Russian)
- [15] A. Sinelshchikov, N. Panasenko, Spectral Analysis of Seismic Impact in the Theory of Seismic Stability of Hoisting Units, *Vestnik ASTU*, Vol. 43, №2, 2008, pp. 27-34 (in Russian).
- [16] *Recommendations on Expert Inspection of Load - Lifting Machines, General Provisions*, RD 10-112-1-04 Standard, 2002 (in Russian)
- [17] S. Poljakov, *Aseismic Building Structures*, Moscow: Vysshiaia Shkola, 1983 (in Russian).
- [18] *Regulations on Arrangement and Safe Operation of Load - Lifting Cranes*, PB10-382-00 Standard, 2000 (in Russian).
- [19] *Equipment of Nuclear Power Plants, A Strength Calculation Under Seismic Action*, RTM 108.020.37-81 Standard, 1981 (in Russian).
- [20] R. W. Clough, J. Penzien, *Dynamics of Structures*, Boston: McGraw-Hill, 1975.
- [21] V. Rasskazovski, I. Aliev, *Seismic Actions on Hydrotechnical and Energy Structures*, Moscow: Nauka, 1981 (in Russian).
- [22] *Nuclear Power Plants – Design Against Seismic Hazards*, ISO 6258-85 Standard, 1985
- [23] *Regulations for Calculation of Load - Lifting Cranes' Spatial Metal Constructions Under Operational and Seismic Actions at Nuclear Power Plants*, RD 24.090.83-87 Standard, 1988 (in Russian).
- [24] A. H. Hadjian, S. F. Masri, A. F. Saud, A Review of Methods of Equivalent Damping Estimation From Experimental Data, *Journal of Pressure Vessel Technology*, Vol. 109, №2, 1987, pp. 236-243.
- [25] A. Ceitlin, About Taking into Account an Internal Friction in Standards on Dynamic Calculation of Structures, *Structural Mechanics and Calculation of Constructions*, №4, 1981, pp. 33-37 (in Russian).
- [26] E. Sorokin, About Inaccuracies of a Well - Known Method in the Theory of Oscillation of Dissipative Systems in Application to Non-Uniform Damping, *Structural Mechanics and Calculation of Constructions*, №2, 1984, pp. 29-34 (in Russian).
- [27] V. Rasskazovski, *Physical Methods Foundations for Determination of Seismic Actions*, Tashkent: Fun, 1973 (in Russian).
- [28] N. Panasenko, S. Bozhko, *Aseismic Lifting-Transport Machines of Nuclear Power Plants*, Krasnoyarsk: KSU, 1987 (in Russian).
- [29] *Regulations on Strength Calculation of Equipment and Pipelines of Nuclear Power Installations*, PNAE G-7-002-86 Standard, 1989 (in Russian).
- [30] V. Slivker, *Structural Mechanics: Basic Variational Principles*, Moscow: ASV, 2005 (in Russian).
- [31] A. Birbraer, S. Shulman, *Strength and Reliability of Constructions of Nuclear Power Plants Under Special Dynamic Loads*, Moscow: Energoatomizdat, 1989 (in Russian).